Proceedings of the 2nd ITB Graduate School Conference ISSN: 2963-718X
Strengthening Multidisciplinary Research to Enhance its Impact on Society
July 21, 2021

Wind flows and pressure on the Joglo roof, one of Indonesia's traditional houses: A simulation and numerical study

Randi Rusdiana, Qhathrin Nada, Rafles Sinaga & Mikrajuddin Abdullah*

Department of Physics, Bandung Institute of Technology, Jalan Ganesa 10, Bandung 40132, Indonesia
*Email: profmikra@gmail.com

Abstract. Joglo is one of the traditional houses in Indonesia. Joglo roof has a different angle. Angle of the Joglo roof is very important to note. In this study, simulated wind with a speed of 10 m/s hitting the Joglo's roof, with roof angles 0º, 35º, 45º, and 55º. The simulation is completed through the Standard k-Epsilon turbulence model with several functions in OpenFOAM and ParaView. First the wind is set in the direction of the x axis and the second is set in all directions towards the horizontal x and y direction, and towards the vertical z direction. The overall flow pattern shows that the velocity gradient towards zero is at the rear of the joglo roof. In unidirectional winds, the highest pressure occurs when the wind bends at a distance of ±45 m. While the lower pressure is on the back of the roof. For wind from all directions, the highest wind speed is at a distance of 7m to 13m. The greater the angle of the Joglo roof, the greater the initial pressure received, and the greater the decrease in pressure value due to the wind being deflected to the vertical z direction.

Keywords: *Joglo's Roof, OpenFOAM, ParaView, and Wind.*

1 Introduction

Indonesia has more than 34 traditional houses with their own characteristics. These characteristics can be located on the stage floor, stairs, walls, and roof. The uniqueness of the traditional house makes the house comfortable to live in, warm, safe from wild animals, and sturdy when strong winds come. One of the traditional houses in Indonesia is the Joglo house, a Javanese traditional house made of teak wood with a pyramid-shaped Joglo roof that refers to the shape of a mountain. In each area, the Joglo house has a roof with a different angle of inclination. The characteristic of the Joglo roof can be seen from the shape of the roof which is a combination of two triangular roof planes with two trapezoidal roof planes, each of which has a different slope angle and is not the same size. The roof of the Joglo is always located in the middle and is always higher and flanked by the roof of the porch. The roof of the Joglo house has a variation of the angle of inclination between 30º to 60º. The angle of the roof slope is an

important thing to consider when building or renovating a Joglo roof. The roof will not function well as a house protector from heat or rain if the angle of inclination is wrong. If it is too sloping, the roof will sag easily and if it is too sloping, the rainwater will not flow smoothly. In addition, the slope of the Joglo roof is predicted to affect wind deflection so that it can withstand the speed and pressure caused by strong winds. Studies on the analysis of the effect of the Joglo roof angle on changes in wind speed and pressure have not been previously reported.

In the last few decades, there have been many studies on simulation and numerical modeling of wind flow on roofs and building shapes. Simulations and modeling use openFOAM to model airflow induced loads on various structures (Isaev et al., 2019; Rajput et al., 2021). Open FOAM has several advantages, such as free access, easy to use, accurate results, and can be used for various purposes related to Computational Fluid Dynamics (CFD). Research that has been carried out includes dynamic simulation of two-phase fluid flow and mass transfer in a forward flow reactor (Nieves-Remacha et al., 2015), simulation of non-premixed turbulent combustion (integration and validation) (Gaikwad & Sreedhara, 2019), flow turbulent buoyant atmosphere over complex geometries (Flores et al., 2013), numerical simulation of viscoelastic two-phase flow (Habla et al., 2011), simulation of airflow inside a horticultural high tunnel greenhouse (Lubitz, 2018), and others.

This paper is structured to determine the effect of the slope angle of the Joglo roof on changes in wind speed and pressure in certain directions. The slope of the angle that is varied is the magnitude of the value of as shown in figure 1.

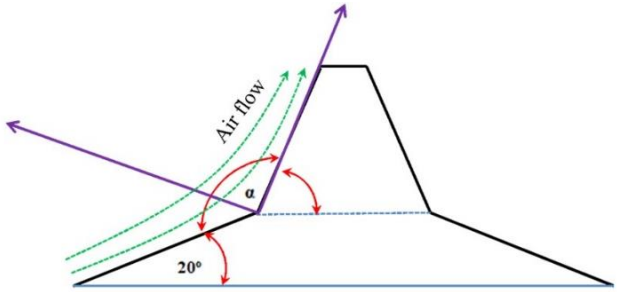

Figure 1. Schematic of the Joglo roof with the value of being a varied angle

Wind flow is simulated using openFOAM software and paraView to display the simulation results. This study is expected to be able to provide information in determining variations in the angle of the roof of the Joglo house so that the house can withstand strong winds or tornadoes.

2 Building Equations and Methods

2.1 Building Equations

Pay attention to the airflow hitting the front side of the roof. For convenience, the coordinate axes are selected as shown in Figure 1. The potential flow around the two walls forms an angle α: (Bird et al., 2002).

$$w(z) = -\beta z^{\alpha} \quad (1)$$

where β is the parameter that determines the wind strength, $z = x + iy$ is a complex variable and $i = \sqrt{-1}$. The complex velocity is derived from the flow potential equation as follows

$$-v_x + iv_y = \frac{dw}{dz} = -\beta\alpha z^{\alpha-1} = -\beta\alpha r^{\alpha-1} e^{i(\alpha-1)\theta}$$

Where $r = \sqrt{x^2 + y^2}$ and $\theta = (y/x)$. From equation (2), it can be determined the velocity component along the x and y coordinates as follows

$v_x = \beta\alpha r^{\alpha-1}\ cos\ cos\ (\alpha - 1)\theta$

and

$v_y = -\beta\alpha r^{\alpha-1}\ sin\ sin\ (\alpha - 1)\theta$

The velocity in the radial direction satisfies the equation:

$v_r = v_x\ cos\ cos\ \theta\ + v_y\ sin\ sin\ \theta$

$v_r = \beta\alpha r^{\alpha-1}\ cos\ cos\ \theta\ \ cos\ cos\ (\alpha - 1)\theta\ - \beta\alpha r^{\alpha-1}\ sin\ sin\ \theta\ \ sin\ sin\ (\alpha - 1)\theta$

$v_r = \beta\alpha r^{\alpha-1}\ cos\ cos\ \alpha\theta$

The magnitude of the total momentum of the left changing direction is the same, because of that,

$$dp = \sqrt{p_r^2 + p_l^2 - 2p_r p_l\ cos\ cos\ (\pi - \pi/\alpha)}$$

$$= \sqrt{p_r^2 + p_l^2 + 2p_r p_l\ cos\ cos\ (\pi/\alpha)}$$

$$= \rho L_R \beta^2 \alpha^2 a^{2\alpha-1} dt\varphi(\alpha)$$

$$\sqrt{1 + (b/a)^{4\alpha-2} + 2(b/a)^{2\alpha-1}\ cos\ cos\ (\pi/\alpha)}$$

If $a \approx b$:

$$p = \rho L_R \beta^2 \alpha^2 a^{2\alpha-1} dt\varphi(\alpha)\sqrt{2}\sqrt{1 + cos\ cos\ (\pi/\alpha)} \quad (2)$$

The force experienced by the Joglo roof can be defined by the equation:

$$F_d = \frac{dp}{dt} \quad (3)$$

If a and b are large enough then we can assume that $p_l \approx p_r$ so that the direction of the Bernoulli force and the force due to bending of air is exactly opposite. Thus, the net upward force received by the roof becomes:

$$F_{nett} = F_B - F_d \quad (4)$$

2.2 Method

OpenFOAM is a free and open source software for Computational Fluid Dynamics (CFD). The workflow in this study is divided into 3 parts, namely: Pre-Processing, Processing, and Post-Processing as shown in figure 2.

Pre-Processing: The Joglo roof geometry was created with the Salome software. Then imported in OpenFOAM. Mesh is created using the tools "blockMesh" and "snappyHexMesh" tools. To complete pre-processing, first define initial conditions and boundary conditions.

Processing: The numerical parameters for the simulation are set according to the Joglo roof problem. Although a problem can be solved through several solving methods, it is very important to choose the appropriate parameters in order to solve the problem efficiently.

Post-Processing: carried out after completing the simulation to interpret the results using the ParaView software. Flow fields can be analyzed by extracting data, plotting, and applying filters such as flowlines and coloring.

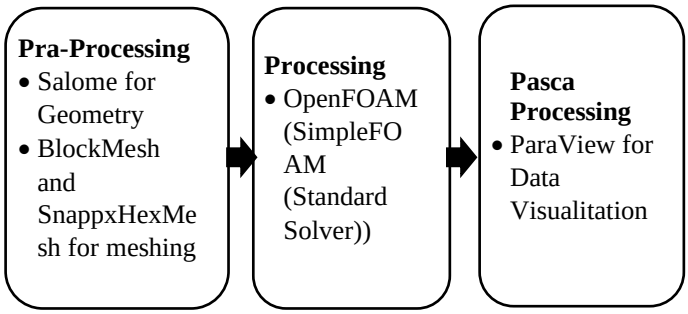

Figure 2. Workflow of simulation.

2.3 Pre-Processing: Creating Geometry and Meshing

The base mesh was created using "blockMesh", then added the Joglo roof mesh using "snappyHexMesh". The Joglo roof geometry used by snappyHexMesh was created in the SALOME-9.7.0 software as shown in Figure 3.

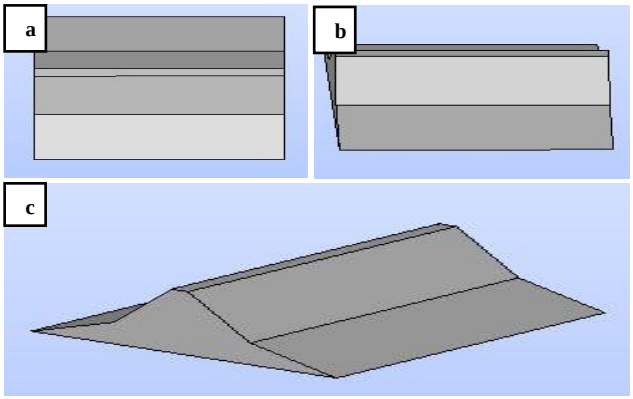

Figure 3. Geometry of the Joglo roof, top view, side and diagonal

2.4 Processing: Solution Using HELYX-OS and OpenFOAM

2.4.1 Boundary Conditions

The general boundary conditions are defined as in the case of a similar CFD (Dwyer 2014) and can be seen in Table 1. In general, the speed on the ground and on the roof of the Joglo is defined with a fixed value of "0", while the other parameters are set to the appropriate Wall-Functions.

The speed at the inlet is set according to the desired inlet wind. In this case, the inlet speed of 10 m/s is used. Meanwhile, the turbulence parameters k, Epsilon (ε) and Omega (ω) are calculated based on the derivation according to the respective turbulence models used. All other values are defined as zero gradient, except for the pressure at the outlet, where a fixed value of "0" is defined to allow free flow of air out.

Table 1 Conditions for the modeling of the joglo roof.

Boundary Condition	**Tipe**	**U**	**P**	**k**	**(ε)**	**nut**
Inlet	Patch	Fixed value	zeroGradient	Fixed Value (calculated)	Fixed Value (calculated)	Fixed Value (calculated)
Outlet	Patch	pressure *Inlet*OutletVelocity	totalPressure	*Inlet*Outlet	*Inlet*Outlet	Fixed Value (calculated)
Ground	Wall	Zero Gradient	Zero Gradient	kqRWall Function	epsilon WallFunction	nutkWall Function
Front	symmetry	Zero Gradient	Zero Gradient	Zero Gradient	Zero Gradient	Zero Gradient

Back	symmetry	Zero Gradient	Zero Gradient	Zero Gradient	Zero Gradient	Zero Gradient
Geometri Atap Joglo	Wall	Fixed Value	Zero Gradient	kqRWall Function	Epsilon-WallFunction	nutkWall Function

2.5 Turbulence and Coefficient Model

Based on the literature review, the Standard k-Epsilon turbulence model (Norton et al. 2007) can be applied to this case. The Standard k-Epsilon model is one of the turbulence models based on the resolution of two additional transport equations for turbulent kinetic energy (k) and dissipation rate (Epsilon) (Launder and Spalding. 1974). The following settings are used for the model, following the default OpenFOAM values as used in the case of other CFDs

Table 2 Standard parameter values for k-Epsilon.

Parameter	Standard k-Epsilon
σ_k	Calculated
σ_ε	Calculated
k	Calculated
Epsilon (ε)	Calculated
C_1	1.44
C_2	1.92
$C\gamma$	0.09

The constants C_1, C_2 , and $C\gamma$ were experimentally determined by (Shih et al. 1994) as C_1 = 1.44, C_2 = 1.92, $C\gamma$ = 0.09 which is the default setting in OpenFOAM. Turbulence coefficient of turbulent kinetic energy (k), turbulence dissipation (ε) and specific turbulence dissipation (ω) were calculated from turbulence intensity (Tu), turbulence length scale (TuL), constant $C\gamma$ and freestream velocity ($U\infty$). The Standard k-Epsilon turbulence model is applied to the four variations of the roof angles of the joglo house

Table 3 Convergence criteria for simulation.

Parameter	Toleran Value
Pressure (p)	$1\ e^{-6}$
Velocity (U)	$1\ e^{-6}$
Turbulent Kinetic Energi (k)	$1\ e^{-6}$
Turbulent Kinetic Energy Dissipation (epsilon)	$1\ e^{-6}$
nuTilda (nut)	$1\ e^{-6}$

ParaView is used to view simulation results and sample data. ParaView provides a GUI and is included with OpenFOAM via the "paraFoam" command. ParaView can display data objects in the form of images or videos. In ParaView, the function object "probe" is used to extract data from a certain point, for example from a certain point the airflow along the roof of a Joglo house is measured using the "volFieldValue" function.

3 Results and Discussion

The overall flow pattern shows that a velocity gradient towards zero is present at the back of the Joglo roof as shown in figure 4. The wind speed is set uniformly at 10 m/s towards the horizontal direction (x axis). At a time of 100 seconds, an increase in speed occurs at a distance of ±50 m after undergoing a turn at a distance of ±45 m as shown in

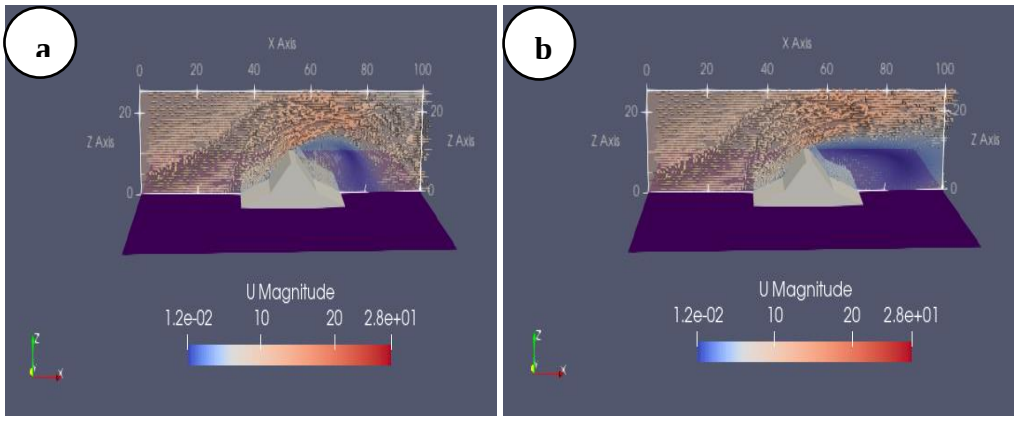

Figure 4: Showing the velocity magnitude of the convergent simulation (k-epsilon turbulence model, Inlet Velocity 10 m/s). 2D View with ParaView uses the "slice" function in the normal Y direction. Roof angle 45 º (a) time 50 seconds, and (b) time 300 seconds.

Figure 4a. The increase in speed occurs up to ±80 m and then starts to stabilize again at a distance of ±85 m. The highest speed value is above the top of the Joglo roof, which is 16.61 m/s at a distance of ±58 m. In this section there is wind that experiences a deflection towards the vertical direction (z axis). Meanwhile, at a time of 300 seconds, an increase in speed occurs at a distance of ±50 m to ±100 m (the very end). The deflection distance of the wind is further than the time of 100 seconds as shown in Figure 4b.

The pressure distribution is shown in figure 5. At a time of 50 seconds an increase in pressure occurs at a distance of ± 45 m when the wind bends as shown in figure 5a. This is indicated by the color gradation that is redder than the other parts.

Similarly, at the time of 300 seconds shown in Figure 5b, the highest pressure occurs when the wind bends. While the lower pressure is on the back of the roof. This is because the wind is deflected towards the vertical (z) direction. The pressure distribution does not change significantly at 100 seconds to 400 seconds. This shows that the longer the pressure will be more stable at a certain amount because the wind speed stabilizes after that time.

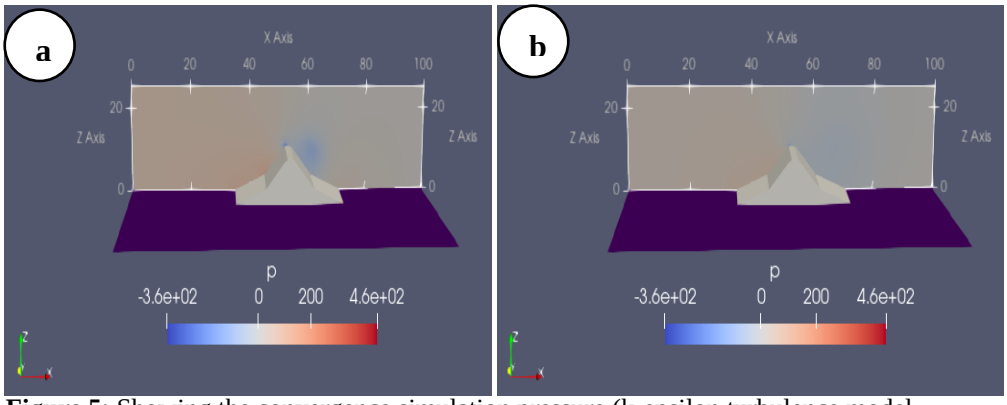

Figure 5: Showing the convergence simulation pressure (k-epsilon turbulence model, entry speed 10 m/s). A 2D View with ParaView uses the "slice" function in the second row in the normal Y direction. Roof angle 45 º. (a) Time 50 seconds and (b) time 300

Significant changes occur at the beginning of the wind towards the roof of the Joglo, which is between time 0 to 50 seconds. In addition to the velocity and pressure in the horizontal direction (x axis), there is also velocity and pressure in the vertical direction (z axis) from the bottom of the Joglo roof to the top. This can cause the roof to lift if the velocity and pressure are very large, or in other words the lifting force is very large. Therefore, in this section, a vertical line is taken to show changes in the value of velocity and pressure at each point as shown by the arrow in Figure 4. This vertical line data is then depicted on a graph as monitoring data. The angles of the Joglo roof are varied to see their effect on changes in velocity and pressure. In this case the angles that are varied are 0 º, 35 º, 45 º and 55 º. Completion of the model is completed through the standard k-Epsilon turbulence model until it reaches certain convergence criteria.

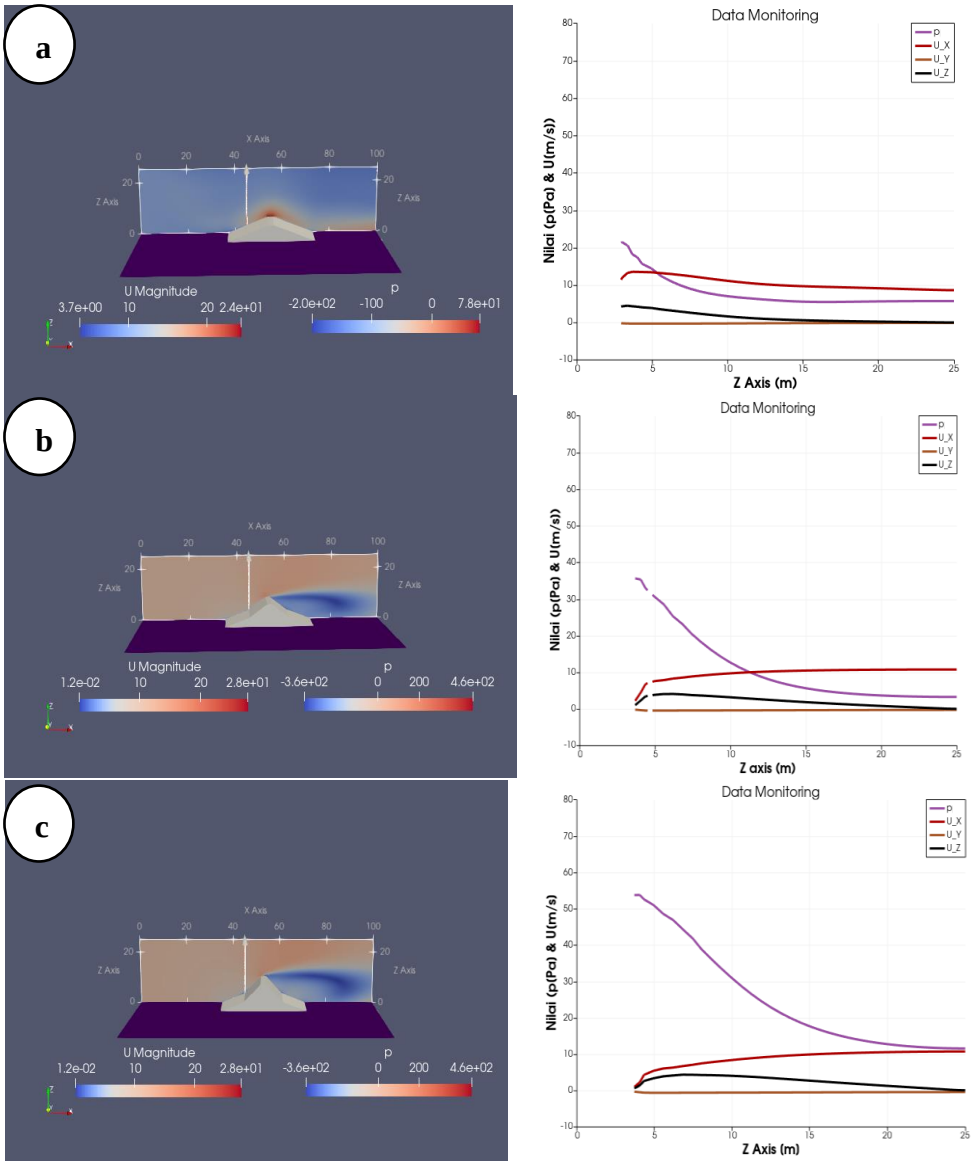
a
b
c
X Axis
Z Axis
U Magnitude
p
3.7e+00
10
20
2.4e+01
-2.0e+02
-100
0
7.8e+01
1.2e-02
2.8e+01
-3.6e+02
200
4.6e+02
Data Monitoring
p
U_X
U_Y
U_Z
Nilai (p(Pa) & U(m/s))
Z Axis (m)
Z axis (m)

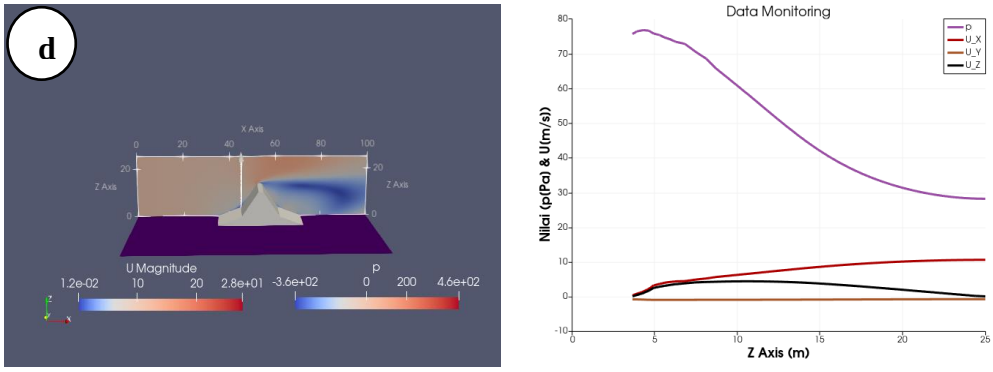

Figure 6. Simulation model and graph of changes in pressure and velocity values in the z direction (z axis) of the Joglo roof where (a) 0º, (b) 35º, (c) 45º, dan (d) 55º

Probes and other simulation data were obtained using pre-configured functions in /system/controlDict as well as some functions in ParaView. The figure shows that there is a difference in the value of the initial pressure received by the roof. The initial pressure received is 21.31 Pa for an angle of 0º, 35.65 Pa for an angle of 35º, 53.77 Pa for an angle of 45º, and 75.77 Pa for an angle of 55º. This shows that the greater the angle of inclination of the Joglo roof, the greater the pressure received. While the final pressure on the boundary conditions section, namely at x: 45, y: 0, and z: 25, is at a value of 5.74 Pa for a 0º slope angle, 3.31 Pa for a 35º slope angle, 11.6 Pa for a 45º angle, and 28.24 for a 55º. The wind speed in the horizontal direction x (U_x) tends to be stable at 10 m/s for an angle of 0º. This is because the incoming wind speed is set to the horizontal x direction and there is no large enough wind deflection. Meanwhile, angles of 35º, 45º and 55º have small wind speeds, namely 2.24 Pa, 1.05 Pa, and 3.86 Pa. This is because the wind is blocked by the roof which is then deflected upwards. There is no velocity in the horizontal y direction. However, in the vertical z direction (U_z) there is a wind speed value due to the deflection of the wind from the x direction to the z direction on the Joglo roof, so that the wind goes vertically upwards. The greatest speed value is at the bottom at the beginning of the deflection of the wind, which is 4.25 Pa.

Table 4 Changes in pressure and velocity values in the vertical direction (z axis) at each corner of the Joglo roof

No	Atap Joglo	Parameter											
		p			U_X			U_Y			U_Z		
		Awal	Akhir	Diff	Awal	Akhir	Diff	Awal	Akhir	Diff	Awal	Akhir	Diff
1	Nol derajat	21.31	5.74	-15.57	11.44	8.65	-2.79	0	0	0	4.25	0	-4.25
2	35 Derajat	35.65	3.31	-32.34	2.24	10.8	8.56	0	0	0	1.08	0.06	-1.02
3	45 Derajat	53.77	11.6	-42.17	1.05	10.76	9.71	0	0	0	0.63	0.12	-.51
4	55 Derajat	75.66	28.24	-47.43	3.86	10.65	6.79	0	0	0	0.11	0.18	.07

Changes in the value of pressure and wind speed from each angle variation are shown in table 4. The greater the angle of the Joglo roof, the greater the decrease in the pressure value in the vertical direction (from bottom to top) as shown in the table in green. This is indicated by the difference between the final pressure and the initial pressure. The large angle of the Joglo roof can reduce the pressure value significantly. The greater the angle of the Joglo roof, the wind speed in the x direction (x axis) will increase up to a 45^{o} angle as shown in blue in table 3 column U_X. Meanwhile, for the 55^{o} angle, the wind speed has decreased. In the vertical direction (z axis), the greater the angle of the Joglo roof, the higher the wind speed as shown in blue in table 1 column U_Z. This indicates that the wind coming from the x direction will soon be deflected towards the z direction so that the wind speed increases. Joglo roof studies through Computational Fluid Dynamic (CFD) can be implemented in OpenFOAM using the Darcy-Forchheimer Equation. Comparison with similar cases from the literature confirms the results (F. D. Molina-Aiz et al. 2012) and (Muñoz, Montero, and Antón 2001). However, it must be said that the results are based on airflow coming mostly from a uniform direction. If you take into account winds that come diagonally, as happens in nature, the results will change (López et al. 2016). No significant change in airflow pattern could be found for the different speeds. Comparison of four models with different Joglo roof angles shows similar flow patterns. The same is true for variations of different angles. If the incoming wind is set from all directions with the same speed value, which is 10 m/s until there is a rotation resembling a tornado, the simulation model is obtained as follows.

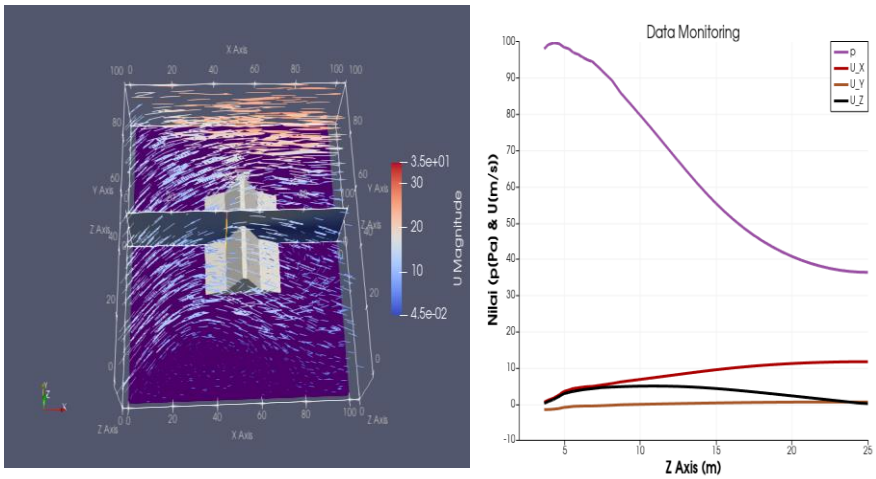

Figure 7. Tornado wind model simulation and graph of changes in pressure and velocity values in the vertical direction (z axis) of the Joglo roof with the k-epsilon turbulence model, the incoming speed is 10 m/s. A 2D View with ParaView uses the "slice" function in the second row in the normal Y direction. Roof angle 55

In this simulation, the wind is set from all directions, namely from the horizontal direction (x axis and y axis) and the vertical direction (z axis) so that the wind rotates as shown in figure 6. Winds that experience rotation are most likely to lift the roof if the speed is high. and the pressure is great. In this section, one line is taken on the slice to see changes in pressure and wind speed in the vertical direction (z axis). The line is indicated by a yellow arrow in figure 4, precisely at points x: 45 m and y: 45 m. Changes in wind speed in the horizontal direction (x axis), the higher the roof will be because there is a driving force from the vertical (z axis) and horizontal (y axis) direction. Meanwhile, for changes in speed in the vertical direction (z axis), the highest wind speed is found in the distance between 7 m to 13 m, precisely on the roof after the wind bends. The initial pressure at the bottom of the Joglo roof is 98.00 Pa and the final pressure at the top of the Joglo roof is 36.37 Pa, so that it has a difference or pressure drop of 61.63 Pa.

The difference value obtained is greater than the change in pressure in a uniform wind direction (see Figure 5 and table). This is due to the large angle of the roof so that it can turn the wind direction quickly and reduce the pressure significantly. Thus, a larger roof angle will be more resistant and stronger against wind pressure than a smaller angle if there are strong winds or tornadoes.

4 Conclusion

The completion of the Joglo roof simulation was completed through the Standard k-Epsilon turbulence model with several functions in OpenFOAM and ParaView. The overall flow pattern shows that the velocity gradient towards zero is at the back of the Joglo roof, with the highest velocity value of 16.61 m/s at a distance of ±58 m. At the wind speed which is set in the direction of x, the highest pressure occurs when the wind bends at a distance of ±45 m. While the lower pressure is on the back of the roof. For wind speeds that are set from all directions, namely the horizontal direction (x axis and y axis) and vertical direction (z axis), the highest wind speed is at a distance of 7 m to 13 m. The initial pressure at the bottom of the Joglo roof is 98.00 Pa and the final pressure at the top of the Joglo roof is 36.37 Pa, with a large difference of 61.63 Pa. The value of the difference is quite large due to the large angle of the roof of the Joglo so that it can turn the wind direction quickly and reduce the pressure significantly. The greater the angle of the Joglo roof, the greater the initial pressure received because the wind is restrained by the vertical roof walls. The presence of wind that is deflected in a vertical direction will reduce the initial pressure value received significantly, so that the greater the angle of the Joglo roof, the lower the pressure value will be even greater. Conversely, the smaller the angle of the Joglo roof, the smaller the initial pressure received will be. The very small corner of the Joglo roof shows the shape of a straight roof in the direction of the wind. This results in no

significant vertical deflection of the wind so that the initial pressure received is small and the pressure drop is also small.

Acknowledgement

The author would like to thank Mr. Mikrajuddin Abdullah for his discussion and guidance as well as his friends in writing scientific papers so that the author can complete this paper.

References

[1] Bird, R. B., Stewart, W. E., & Lightfoot, E. N., Transport Phenomena, *Revised 2nd Edition*. *John Wiley*, 2002.

[2] Flores, F., Garreaud, R., & Muñoz, R. C., CFD simulations of turbulent buoyant atmospheric flows over complex geometry: *Solver development in OpenFOAM*. *Computers and Fluids*, **82**, pp. 1–13, 2013. https://doi.org/10.1016/j.compfluid.2013.04.029.

[3] Gaikwad, P., & Sreedhara, S., OpenFOAM based conditional moment closure (CMC) model for solving non-premixed turbulent combustion: Integration and validation. *Computers and Fluids*, vol. 190, 362–373, 2019. https://doi.org/10.1016/j.compfluid.2019.06.029.

[4] Habla, F., Marschall, H., Hinrichsen, O., Dietsche, L., Jasak, H., & Favero, J.L., Numerical simulation of viscoelastic two-phase flows using openFOAM®. *Chemical Engineering Science*, vol. 66, no. 22, pp. 5487–5496, 2011. https://doi.org/10.1016/j.ces.2011.06.076.

[5] Isaev, S. A., Gritckevich, M. S., Leontiev, A. I., Milman, O. O., & Nikushchenko, D. V., NT Vortex enhancement of heat transfer and flow in the narrow channel with a dense packing of inclined one-row oval-trench dimples. *International Journal of Heat and Mass Transfer*, vol. 145, 118737, 2019. https://doi.org/10.1016/j.ijheatmasstransfer.2019.118737.

[6] Launder, B.., & Spalding, D., The numerical computation of turbulent flows. *Computer Methods in Applied Mechanics and Engineering*, vol. 3, no. 2, pp. 269–289., 1974. https://doi.org/https://doi.org/10.1016/0045-7825(74)90029-2.

[7] López, A., Molina-Aiz, F. D., Valera, D. L., & Peña, A., Wind tunnel analysis of the airflow through insect-proof screens and comparison of their effect when installed in a mediterranean greenhouse. *Sensors (Switzerland)*, vol. 16, no. 5, pp. 5–8, 2016. https://doi.org/10.3390/s16050690.

[8] Lubitz, W., & Hopf, A., Simulation of airflow within horticulture high-tunnel greenhouses using open-source CFD software. *Hochschule Geisenheim University, Germany*, 2018.

[9] Molina-Aiz, F. D., Valera, D. L., López, A., Álvarez, A. J., & Escamirosa, C., Effects of insect-proof screens used in greenhouse on microclimate and fruit yield of tomato (Solanum lycopersicum L.) in a mediterranean climate. *Acta Horticulturae*, vol. 927, pp. 707–714, 2012. https://doi.org/10.17660/ActaHortic.2012.927.88.

[10] Muñoz, P., Montero, J. I., & Antón, A., Natural Ventilation of multi-span tunnel greenhouses with and without insect-proof screen. *International Symposium on Protected Cultivation in Mild Winter Climates: Current Trends for Suistainable Technologies*, vol. 559, pp. 263–270, 2000.

[11] Nieves-Remacha, M. J., Yang, L., & Jensen, K. F., OpenFOAM Computational Fluid Dynamic Simulations of Two-Phase Flow and Mass Transfer in an Advanced-Flow Reactor. Industrial and Engineering Chemistry Research, vol. 54, no. 26, pp. 6649–6659, 2015. https://doi.org/10.1021/acs.iecr.5b00480.

[12] Norton, T., Sun, D. W., Grant, J., Fallon, R., & Dodd, V., Applications of computational fluid dynamics (CFD) in the modelling and design of ventilation systems in the agricultural industry: A review. *Bioresource Technology*, vol. 98, no. 12, 2386–2414, 2007. https://doi.org/10.1016/j.biortech.2006.11.025.

[13] Rajput, M., Augenbroe, G., Stone, B., Georgescu, M., Broadbent, A., Krayenhoff, S., & Mallen, E. (2021). Heat exposure during a power outage: A simulation study of residences across the metro Phoenix area. Energy and Buildings, xxxx, 111605. https://doi.org/10.1016/j.enbuild.2021.111605.